infrastructures

MDPI

Article

Physical, Mechanical and Durability Properties of Eco-Friendly Engineered Geopolymer Composites

Ahmed M. Tahwia [1,*], Duaa S. Aldulaimi [1], Mohamed Abdellatief [2] and Osama Youssf [1]

[1] Structural Engineering Department, Faculty of Engineering, Mansoura University, Mansoura 35516, Egypt; duaa.salah@std.mans.edu.eg (D.S.A.); osama.youssf@mymail.unisa.edu.au (O.Y.)
[2] Department of Civil Engineering, Higher Future Institute of Engineering and Technology, Mansoura 35516, Egypt; besttime703@std.mans.edu.eg
* Correspondence: atahwia@mans.edu.eg

Abstract: Engineered geopolymer composite (EGC) is a high-performance material with enhanced mechanical and durability capabilities. Ground granulated blast furnace slag (GGBFS) and silica fume (SF) are common binder materials in producing EGC. However, due to the scarcity and high cost of these materials in some countries, sustainable alternatives are needed. This research focused on producing eco-friendly EGC made of cheaper and more common pozzolanic waste materials that are rich in aluminum and silicon. Rice husk ash (RHA), granite waste powder (GWP), and volcanic pumice powder (VPP) were used as partial substitutions (10–50%) of GGBFS in EGC. The effects of these wastes on workability, unit weight, compressive strength, tensile strength, flexural strength, water absorption, and porosity of EGC were examined. The residual compressive strength of the proposed EGC mixtures at high elevated temperatures (200, 400, and 600 °C) was also evaluated. Additionally, scanning electron microscope (SEM) was employed to analyze the EGC microstructure characteristics. The experimental results demonstrated that replacing GGBFS with RHA and GWP at high replacement ratios decreased EGC workability by up to 23.1% and 30.8%, respectively, while 50% VPP improved EGC workability by up to 38.5%. EGC mixtures made with 30% RHA, 20% GWP, or 10% VPP showed the optimal results in which they exhibited the highest compressive, tensile, and flexural strengths, as well as the highest residual compressive strength when exposed to high elevated temperatures. The water absorption and porosity increased by up to 106.1% and 75.1%, respectively, when using RHA; increased by up to 23.2% and 18.6%, respectively, when using GWP; and decreased by up to 24.7% and 22.6%, respectively, when using VPP in EGC.

Keywords: eco-friendly; engineered geopolymer composite; rice husk ash; granite waste powder; volcanic pumice powder

Citation: Tahwia, A.M.; Aldulaimi, D.S.; Abdellatief, M.; Youssf, O. Physical, Mechanical and Durability Properties of Eco-Friendly Engineered Geopolymer Composites. *Infrastructures* **2024**, *9*, 191. https://doi.org/10.3390/infrastructures9110191

Academic Editors: Patricia Kara De Maeijer and Pedro Arias-Sánchez

Received: 29 September 2024
Revised: 18 October 2024
Accepted: 24 October 2024
Published: 25 October 2024

1. Introduction

Concrete is the most utilized material for construction in the world, with a tensile strain capacity of about 0.01%. It is strong in compression but weak in tension [1]. Since the 1960s, a variety of studies have concentrated on developing fiber-reinforced cementitious composites in an attempt to counteract this weakness [2]. Early in the 1990s, researchers developed engineered cementitious composites (ECCs), which have exceptional tensile ductility and multiple cracking characteristics that can overcome the brittleness of regular cementitious materials [1]. However, the typical ECC mix usually requires a cement amount that is two to three times more than that required in conventional concrete [3]. The production of ECC releases 8% of world carbon dioxide (CO_2) emissions [4,5]. As a result, in recent decades, a number of studies have concentrated on the production of greener and more sustainable ECCs.

Industrial byproducts that are alkali-activated to create geopolymers are thought to be a viable substitute for Portland cement because of their superior technical qualities

and reduced carbon emissions [6,7]. Geopolymer has been recognized as one of the most promising new green cementitious materials. It is environmentally and economically friendly and has a short setting time, early strength, high-temperature tolerance, and good corrosion resistance [8,9]. Natural minerals or industrial wastes like fly ash, metakaolin, ground granulated blast furnace slag (GGBFS), and rice husk ash (RHA) are typically precursors of geopolymers. These materials are rich in aluminum and silicon and can chemically react with alkaline activators like sodium hydroxide (SH), sodium silicate (SS), and sodium carbonate [10,11]. Given the potential benefit of utilizing geopolymers in the field of concrete construction, numerous attempts have been made to replace Portland cement in ECC with geopolymers to create engineered geopolymer composites (EGCs). EGC is a fiber-reinforced geopolymer composite that is highly ductile, environmentally friendly, and sustainable [12]. Because of their exceptional strength, durability in hard environmental conditions, and friendliness to the environment, these composites are becoming more and more popular in the infrastructure and construction sectors. The EGCs were able to show enhanced mechanical characteristics under dynamic stress but similar tension and flexural characteristics under static loads, thus rendering it a more sustainable material than ECC [12].

Several previous studies have been conducted to develop more sustainable EGCs by applying longer curing periods and higher curing temperatures or utilizing various kinds of alkaline activators and precursors. Wang et al. [13] studied the utilization of recycled concrete powder (RCP) and recycled fine sand (RFS) and found that the addition of RCP slightly improved the flowability. While the inclusion of RFS had the opposite effect, the decrease in flowability induced by RFS was minimized by the combined use of RCP and RFS; this also applied to the setting time and water absorption.

Nematollahi et al. [14] investigated how strain hardening performance for polyvinyl alcohol fiber (PVA) EGC was affected by alkali activator solutions. They tried four types of alkali activators, namely a potassium-based alkali activator liquid, two varieties of SS liquids, and a lime-based activator in powder form. Their results showed that utilizing an SS-based activator and 8M SH liquid with a mixing ratio (SS/SH) of two was extremely advantageous in terms of cost reduction and it showed an EGC tensile strength of 4.7 MPa and compressive strength of 60 MPa. In addition, this alkali activator enhanced the fracture toughness and other matrix fracture parameters. Other researchers studied the impact of various factors on EGC behavior, including the matrix design [15], the combination of superplasticizers and activators [16], the curing temperature [17], and various fly ash and slag ratios.

Yazan and Dai [18] evaluated the impact of fiber hybridization on the tensile characteristics and microstructure of EGCs that were cured at room temperature. The research team discovered that while the EGC hybrid composites' compressive strength, fracture properties, relative slump, and dry density all increased with the addition of steel fiber, the multiple cracking actions and tensile strain capacity were significantly reduced. Additionally, even though the fiber bridging stress and fracture properties were improved, the addition of micro-silica sand dramatically decreased the multiple cracking behaviors and the tensile ductility of EGC composites. Ling et al. [19] reported the effect of slag content on the mechanical properties and bond strength of fly ash EGC. They evaluated the compressive strength, pullout bond strength, flexural strength, tensile properties, and elastic modulus of EGCs when substituting fly ash binder by slag at several weight ratios (0%, 10%, 20%, and 30%). The findings showed that fly ash EGC without slag had low fracture toughness and tensile strain ductility, whereas all EGCs made with slag had superior compressive strength, elastic modulus, initial cracking strength, and fiber bridging stress. Moreover, under uniaxial tensile and flexural loadings, many tiny cracks were seen in all EGC specimens (with and without slag). As the slag percentage of EGCs grew, the number of cracks decreased and their spacing increased. Deb et al. [20] investigated whether the slag and activator contents affect the workability and strength characteristics of fly ash-based geopolymer concrete. They discovered that at all ages up to 180 days, the compressive

strength of the slag-fly ash geopolymer increased with increasing slag content. Ahmed et al. [21] studied replacing slag with recycled brick waste powder (RBWP) and found that the amount of RBWP in the EGC mixture progressively raised water absorption, which reached 304% when slag was completely substituted. The porous surface of unreacted RBWP may be the cause of the increase in water absorption in the mixture of EGC with a high RBWP concentration. Wu et al. [22] studied the incorporation of recycled concrete powder (RCP) and recycled paste powder (RPP) as a substitute for FA-slag EGC and found that the water-permeable porosity and water absorption were increased by incorporating RCP up to 100% as a substitute for FA-slag. The substitution of RCP for FA-slag increases the porosity and associated water transport in EGC because it has low alkali-activated activity and substantial inert components. A noteworthy increase in water absorption and water-permeable porosity is seen, particularly for the fully recycled powder EGC manufactured with 100% RCP. Also, it was found that the water absorption and water-permeable porosity of EGC are not considerably increased when 50% or 100% of FA-slag is replaced with RPP; however, these parameters are greatly increased when 75–100% of FA-slag is replaced with RPP.

With the significant scientific development that has occurred in slag geopolymer composites, the market price of slag has gradually increased. As a result, industrial wastes that are high in silicon and aluminum have turned into a hotspot for research. Therefore, a variety of alternative materials are needed to replace slag in EGC. Rice husk ash (RHA) is a dark powder made by burning rice husks that is a non-environmentally friendly material [23]. It has been reported that using RHA in cementitious composites improved their mechanical properties and reduced their water absorption [24]. Zhao et al. [8] studied the effect of RHA at high content (50–80%) on concrete compressive strength, flexural strength, moisture absorption coefficient and water absorption, and found that 60% RHA and 40% slag can be used together as raw materials to obtain the preferred mechanical properties. Granite waste powder (GWP) is produced during the processing and cutting of granite stone. Using GWP in the construction industry can address many environmental issues related to waste disposal and serve as a tool for resource conservation. It has been shown that GWP can be used as a binder in cementitious composites technology. Filling up the gaps in the cementitious composites' matrix with GWP significantly improves the volume porosity and increases the composites' durability [25]. The demand for natural resources can be decreased by substituting GWP for natural materials like cement and sand. Additionally, industries can save money on raw material costs and develop their circular economy by using GWP to replace a portion of their material requirements [26]. Shilar et al. [27] investigated the optimum percentage of GWP as a binder, studied the effect of the molarity-to-binder ratio on the mechanical properties of geopolymer concrete, and concluded that at 16 M, the maximum compressive, tensile, and flexural strengths were obtained with GWP of 20% content. Volcanic pumice powder (VPP) is a fine, lightweight, and porous material derived from volcanic pumice, which is a type of volcanic rock. Because of its potential as a sustainable substitute for conventional building materials, it has attracted interest in the field of geopolymer research. VPP can improve the mechanical characteristics of geopolymer formulations, giving the material more strength and endurance. Since VPP is a naturally occurring substance that can be sourced responsibly, it is also environmentally beneficial. Because of its abundance and lightweight nature, it presents a promising alternative to the environmentally friendly building techniques [28]. Kabay et al. [29] evaluated the physical, mechanical and microstructural properties of geopolymer pastes and mortars manufactured from VPP and GGBFS with sodium hydroxide, potassium hydroxide, and sodium silicate solution. Their results revealed that the ratio of VPP and the activator concentration have an important role in the compressive strength of pastes.

This research focused on producing more sustainable and eco-friendly EGC made of cheaper and more common pozzolanic waste materials, namely RHA, GWP, and VPP. These waste materials were used as partial substitutions (10–50%) of GGBFS in EGC. The effects of these wastes on workability, unit weight, compressive strength, tensile strength,

flexural strength, water absorption, and porosity of EGC were examined through sixteen proposed mixtures. The residual compressive strength of the proposed EGC mixtures when exposed to high elevated temperatures (200, 400, and 600 °C) and the microstructure of selected mixtures were also evaluated.

2. Experimental Procedures

2.1. Raw Materials and Mix Proportions

A total of sixteen mixtures were designed and tested in this study. The precursor materials utilized in the control EGC mixture of this research included GGBFS and silica fume (SF). The specific gravity of GGBFS and SF were 2.87 and 2.15, respectively. The slag was partially replaced by RHA, GWP, or VPP at 10–50% by volume; while SF was used with constant content in all mixtures. The specific gravities of RHA, GWP and VPP were 1.95, 2.8, and 2.17, respectively. The chemical compositions of all binder materials used are shown in Table 1. A constant content of sand was used as the fine aggregate in all mixtures. The sand had a specific gravity of 2.65, a fineness modulus of 2.20, and a unit weight of 1420 kg/m^3.

A mix of SH and SS solutions was used as the alkaline activator of EGC mixtures. The SH solution with specific gravity of 2.13 was prepared with a molar concentration of 14 M using SH pellets of 97–98% purity locally purchased and dissolved in portable water (dissolving 560 gm of SH pellets in every 1 L of water) and then left in room temperature for 2 h. The prepared SH solution was then mixed with the SS solution (specific gravity of 1.5) for 30 min using a mechanical liquid stirrer. The alkaline activator was then covered and left for 24 h before using in EGC mixing. The weight mixing ratio of SS to SH was kept constant at a value of 2.0.

To control the workability of the proposed EGC mixtures, extra water with 5% binder and superplasticizer (SP) with 1.5% binder were added. The SP had a commercial name of "Sika ViscoCrete ®–3425" type F with specific gravity of 1.15 according to ASTM C494/C494M−17 [30]. Curved wave polypropylene (PP) macro fibers, as shown in Figure 1, with a specific gravity of 0.91 were used to reinforce EGC mixtures. Table 2 lists the characteristics of PP fibers, as provided by the supplier.

The proportions of GGBFS and SF in control EGC precursor materials were 85% and 15%, respectively, and the ratio of the alkaline solution to precursor materials was held constant at 0.4. The volume content of PP fiber remained at 2%. All materials used and the mixing method are shown in Figure 2. Table 3 lists the proportions of the designed EGC mixtures. In this table, EGC refers to the control mix, and RHA, GWP, and VPP refer to mixes including rice husk ash, granite waste powder, and volcanic pumice powder, respectively, as partial replacements of slag followed by the replacement ratio by volume. The replacements in the designed mixes have been carried out by volume to ensure constant absolute volume (1 m^3) for all comparable mixes.

Figure 1. Polypropylene fibers used.

Table 1. Chemical composition of geopolymer precursors.

Geopolymer Precursors	SiO_2 (%)	CaO (%)	Al_2O_3 (%)	Fe_2O_3 (%)	SO_3 (%)	MgO (%)	Na_2O (%)	K_2O (%)	SrO (%)	TiO_2 (%)	P_2O_5 (%)	Mn_2O_3 (%)	LOI (%)
GGBFS	39.8	41.1	11.4	0.4	1.7	3.5	0.4	0.3	0.8	0.6	0.01	0.0	0.8
SF	97.5	0.3	0.2	0.3	0.0	0.6	0.5	0.6	0.0	0.0	0.0	0.0	5.1
RHA	90.14	0.97	3.88	1.15	0.05	0.26	1.39	1.24	0.0	0.0	0.91	0.0	6.13
GWP	69.7	3.6	13.03	3.04	0.28	0.79	3.66	5.29	0.0	0.42	0.09	0.0	0.65
VPP	49.4	7.76	16.87	14.04	0.54	6.01	2.21	2.01	0.0	0.0	0.72	0.19	2.21

Table 2. Physical and mechanical characteristics of macro-PP fibers.

Property	Value
Compressive Strength	550 MPa
Tensile Strength	560 MPa
Modulus of Elasticity	5 GPa
Crack Elongation (%)	≥15
Melting Point	160–170 °C
Length	30 mm
Thickness	0.3 mm
Aspect Ratio	100
Density	910 kg/m^3

Figure 2. Materials and mixing method used in this study.

Table 3. Mix proportions of EGC (kg/m^3).

Mix ID	Precursors					Sand	AAS		SP	Extra Water	PP
	GGBS	SF	RHA	GWP	VPP		SS	SH			
EGC	996.0	118	0	0	0	570	297	148.5	16.71	55.7	18
RHA-10	896.4	118	67.6	0	0	570	297	148.5	16.71	55.7	18
RHA-20	796.8	118	135.3	0	0	570	297	148.5	16.71	55.7	18
RHA-30	697.2	118	203.0	0	0	570	297	148.5	16.71	55.7	18
RHA-40	597.6	118	270.6	0	0	570	297	148.5	16.71	55.7	18
RHA-50	498.0	118	338.3	0	0	570	297	148.5	16.71	55.7	18
GWP-10	896.4	118	0	97.1	0	570	297	148.5	16.71	55.7	18
GWP-20	796.8	118	0	194.3	0	570	297	148.5	16.71	55.7	18
GWP-30	697.2	118	0	291.5	0	570	297	148.5	16.71	55.7	18
GWP-40	597.6	118	0	388.6	0	570	297	148.5	16.71	55.7	18
GWP-50	498.0	118	0	485.8	0	570	297	148.5	16.71	55.7	18
VPP-10	896.4	118	0	0	75.3	570	297	148.5	16.71	55.7	18
VPP-20	796.8	118	0	0	150.6	570	297	148.5	16.71	55.7	18
VPP-30	697.2	118	0	0	225.9	570	297	148.5	16.71	55.7	18
VPP-40	597.6	118	0	0	301.2	570	297	148.5	16.71	55.7	18
VPP-50	498.0	118	0	0	376.5	570	297	148.5	16.71	55.7	18

2.2. Mixing and Curing

All the solid materials (GGBS, SF, sand, and RHA/GWP/VPP) were mixed dry for two minutes. After that, the alkaline activator solution, SP, and extra water were added and mixed for another three minutes. The PP fibers were subsequently added, progressively, evenly distributed, and mixed for another three minutes. The produced EGC was poured into the molds for different tests, and the specimens were subsequently compacted using a vibrating table for ten seconds at a frequency of 3600 vpm. The specimens were kept for 24 h before demolding and cured for another 24 h in an oven at 80 °C, as shown in Figure 3. The specimens were then kept in air after completing the heat-curing process until performing the planned tests. It is worth noting that although heat curing has some practicality and environmental concerns, it is a very effective method of curing for EGC, especially in the very early stages. However, with the recent huge boom in the manufacturing and use of solar cells, more practical and environmentally friendly heat curing of geopolymer concrete and ECC can be applied. Dong et al. [31] have successfully cured geopolymer concrete using the solar curing method and were able to easily reach a 65 °C curing temperature while showing a substantial improvement in the compressive strength.

Figure 3. Heat curing of EGC specimens for 24 h after demolding.

2.3. Test Methods and Specimens Preparation

2.3.1. Workability

The slump and flow diameter tests were conducted for the fresh properties of EGC by taking a sample of fresh EGC immediately after mixing, as shown in Figure 4. The tests were conducted according to AS 1012.3.5 [32]. The mean flow diameter value of EGC was determined by measuring two perpendicular diameters of the material.

Figure 4. Measuring of EGC workability.

2.3.2. Unit Weight

Unit weight tests were conducted for the physical properties of EGC. Prior to conducting the compressive strength test on EGC cubes at 28 days, the unit weight of each EGC mixture was measured by dividing the mass of the cube by the volume.

2.3.3. Mechanical Properties

Compressive Strength

Compressive strength was evaluated in accordance with ASTM C-109 [33] at three EGC ages, namely 7, 28, and 56 days. Nine cubes sized 70 × 70 × 70 mm were cast (three cubes per measurement age), three specimens from each mixture were tested, and the average results were compared.

Tensile Strength

Uniaxial tensile test was performed using dog bone specimens, as shown in Figure 5, in accordance with the guidelines provided by the Japan Society of Civil Engineers [34]. Three specimens from each mix were tested at 28 days, and the average results were compared. Figure 6a describes the uniaxial tensile test setup.

Flexural Strength

A four-point flexural test was carried out at 28 days on EGC plate specimens in accordance with ASTM C1609 [35], as shown in Figure 5. Then, 400 × 100 × 20 mm plates were cast to measure flexural strength (three per mixture). The detailed setup for the four-point flexural tests is shown in Figure 6b. Three specimens were tested, and the average results were compared.

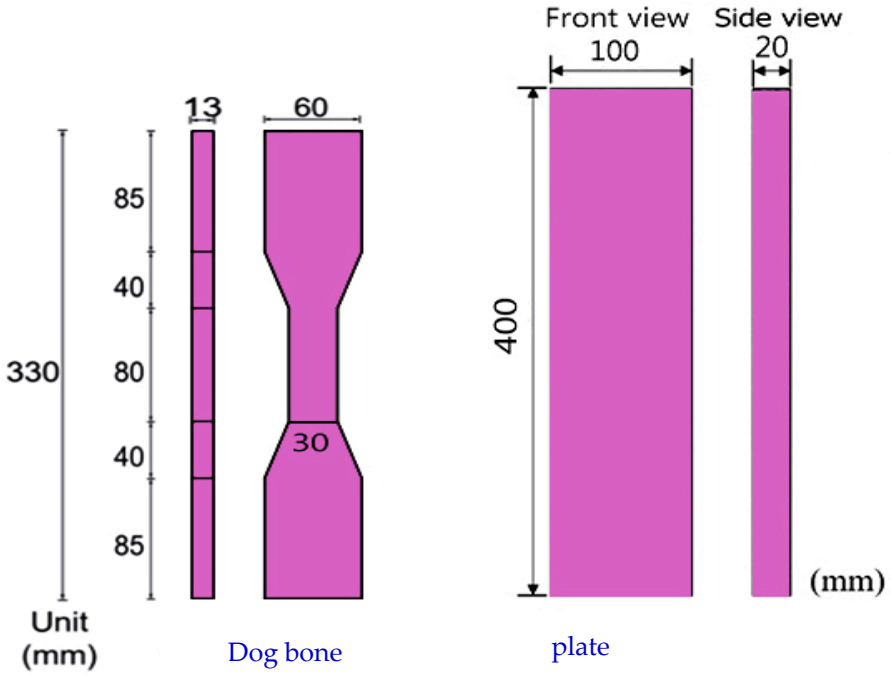

Figure 5. Dimensions of EGC dog-bone and plate specimens.

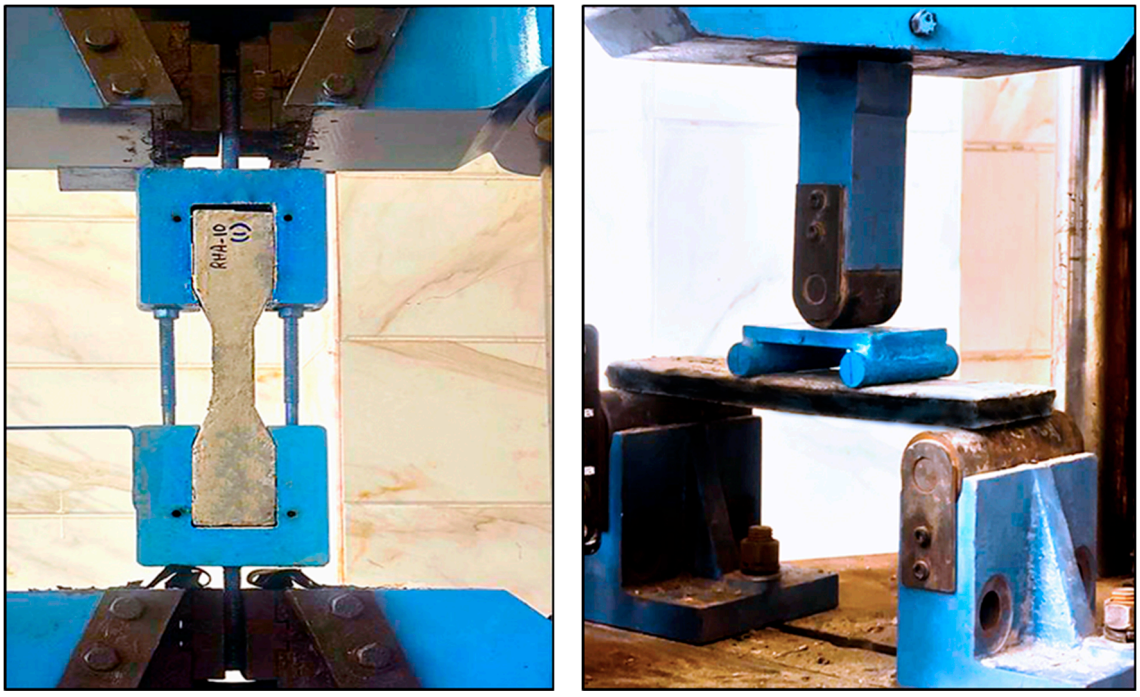

(**a**) (**b**)

Figure 6. Mechanical test setups of EGC: (**a**) Uniaxial tensile test setup, (**b**) Four-point flexural test setup.

2.3.4. Water Absorption and Apparent Porosity

Water absorption and porosity are important properties that express the durability of the structure. The test was carried out according to ASTM C 948 [36]. At the age of 56, three cube specimens sized 70 × 70 × 70 mm of each mixture were soaked in water for 24 h at a temperature of 21 °C. The weight of the fully saturated specimens was measured as "A". After that, the specimens were removed from the water, the surface was dried with a towel, and the weight of the saturated specimens was measured in air as "B". The

specimens were then dried in an oven at a temperature of 100–110 °C for 24 h. After removing them from the oven, the specimens were left to cool down to room temperature, and their weights were measured as "*C*". The water absorption and apparent porosity values were determined using the following equations:

$$\text{Water absorption } (\%) = \frac{B - C}{C} \times 100 \quad (1)$$

$$\text{Apparent porosity } (\%) = \frac{B - C}{B - A} \times 100 \quad (2)$$

where A = immersed mass (g), B = saturated-surface-dry mass (g), and C = oven-dry mass (g).

2.3.5. Residual Compressive Strength

At 28 days, nine cubes sized 70 × 70 × 70 mm of each mixture were used to gauge the resistance to high temperatures (three per temperature level of 200, 400, and 600 °C), placed in an electric oven with a capacity of 1200 °C, and subjected to different elevated temperatures (200, 400, and 600 °C) for two hours. Following heating, the specimens were allowed to cool down to room temperature for 24 h inside the oven to prevent thermal shock, and the residual compressive strength was then measured.

2.3.6. Microstructure Analysis

Scanning electron microscopy (SEM) analysis was carried out on 1 × 1 cm cut pieces that were obtained from the core of the fractured cubic specimens following the compressive strength test to investigate the microstructure of selected EGC mixtures. SEM analysis was performed on the control EGC mixture and optimum mixtures that showed the highest 28-day compressive strength, namely EGC, RHA-30, GPW-20, and VPP-10. The microscope used for the SEM analysis was a QUANTA FEG 250 device with an accelerating voltage of 20 kV.

3. Results and Discussions

Table 4 exhibits the outcomes of the measurements carried out on the EGC mixtures, namely workability (slump and flow diameter), unit weight, compressive strength, tensile strength, flexural strength, water absorption, and apparent porosity.

Table 4. EGC tests result.

MIX ID	Slump (mm)	Flow Diameter (mm)	Unit Weight (kg/m^3)	Compressive Strength (MPa)			Tensile Strength (MPa)	Flexural Strength (MPa)	Water Absorption (%)	Apparent Porosity (%)
				7 D	28 D	56 D				
EGC	65	135	2128	75	78	79	4.5	6.0	6.88	13.44
RHA-10	62	131	2122	52	57	54	3.5	5.5	7.49	14.42
RHA-20	58	126	2118	50	61	48	3.6	5.7	8.62	16.08
RHA-30	54.5	118	2073	55	65	62	4.5	6.2	8.80	16.50
RHA-40	53	115	2007	49	53	51	4.1	5.0	10.44	18.07
RHA-50	50	110	1950	42	44	43	4.0	4.8	14.18	23.54
GWP-10	85	140	2114	52	55	57	4.0	6.3	6.90	13.50
GWP-20	65	135	2099	53	65	69	5.6	6.9	6.94	13.57
GWP-30	50	130	2093	51	53	55	4.9	6.5	8.09	15.22
GWP-40	48	118	2085	52	54	66	4.4	6.4	8.14	15.45
GWP-50	45	116	2067	43	48	53	3.5	6.2	8.48	15.95
VPP-10	55	132.5	2134	52	60	67	4.4	6.6	6.80	13.40
VPP-20	60	134	2152	51	53	57	4.0	6.0	5.56	10.68
VPP-30	75	140	2166	49	50	55	3.5	5.8	5.32	10.51
VPP-40	80	144	2199	46	47	54	3.1	5.1	5.28	10.48
VPP-50	90	160	2269	41	42	50	2.8	4.8	5.18	10.40

3.1. Workability

Figure 7 shows the results of EGC slump and flow diameter. It was observed that the slump and flow diameter of the control EGC were 65 mm and 135 mm, respectively. When partially replacing the EGC slag with RHA at a rate of 10–50%, it was noted that the higher the replacement rate, the lower the workability of the EGC compared to the control mixture, until it reached the lowest workability in mixture RHA-50. Using 50% RHA decreased the EGC slump by 23% and the flow diameter by 18.5%. The reason for the workability decrease when using RHA is attributed to its high absorption rate and large surface area [37]. This decreased the amount of free water within the EGC matrix, and hence, resulted in lower workability. A similar observation was found by Das et al. [38]. Also, Patel and Shah [39] highlighted that workability decreased with an increase in RHA content for the same reasons mentioned above.

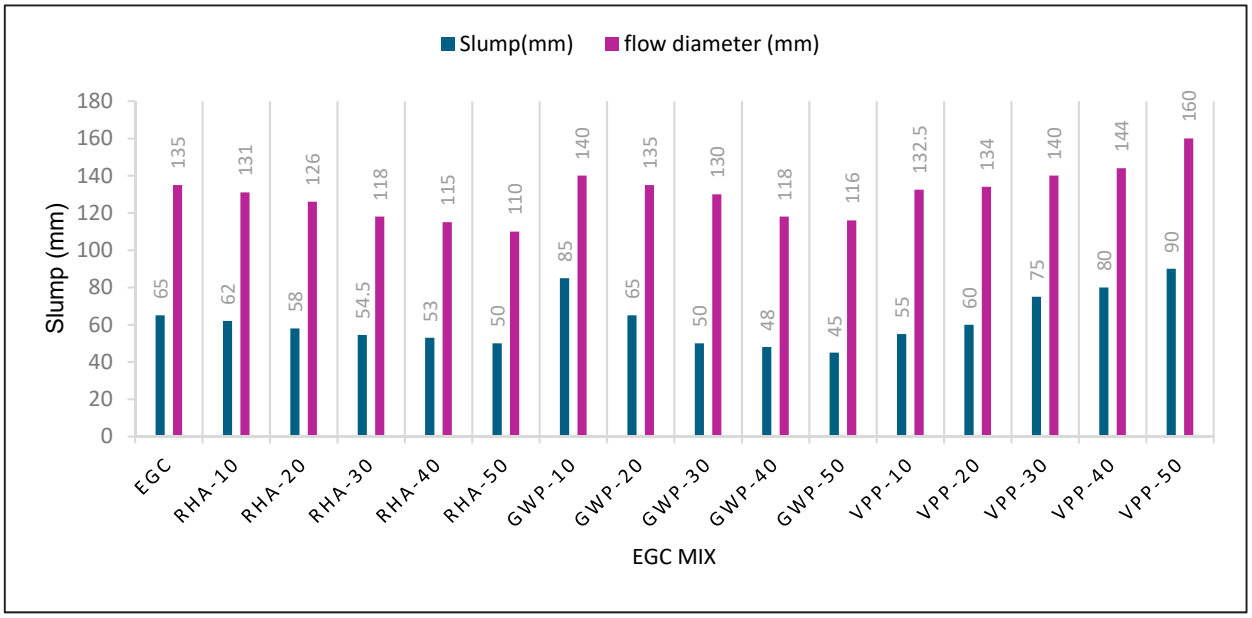

Figure 7. Workability of EGC.

When replacing slag with GWP in the same proportions of 10–50%, an increase in EGC workability was observed at a GWP ratio of 10% (GWP-10 mixture) in which the slump increased by 31% and the flow diameter increased by 4%. At 20% GWP, the workability was similar to that of the control EGC. However, it began to decrease gradually to the lowest value recorded in the GWP-50 mixture. Using 50% GWP decreased the EGC slump by 31% and the flow diameter by 14%. The workability increase at low levels of GWP and decrease at high levels of GWP are due to the irregular shape of GWP particles, which adversely affected the movability of the EGC matrix, and hence, resulted in lower workability. In addition, the high viscosity of the GWP slurry at high contents made the EGC sticky and less workable. Similar results were reported by Shilar et al. [27].

Replacing slag with VPP at the rate of 10% and 20% led to a decrease in EGC workability, compared to the control mixture. At 10% and 20% VPP, the EGC slump decreased by 15% and 8%, respectively, and the flow diameter decreased slightly by 2% and 1%, respectively. Beyond 20% VPP, the workability losses started to recover until it recorded its highest value in mixture VPP-50. Using 50% VPP increased the EGC slump by 38% and the flow diameter by 18%. This might happen because VPP has an uneven, porous particle form and a cellular structure. This may cause the EGC mixture to pack unevenly at low replacement rates, which would make it less workable. Nonetheless, the lubricating action of VPP became more pronounced at high contents, which lessened the particle friction and hence improved the EGC workability. Furthermore, the low weight of VPP could also

contribute to the formation of a more cohesive and stable mixture that enhanced the EGC's overall workability.

In conclusion, 10% GWP provides the most promising results in terms of enhanced workability, with a noticeable improvement in slump and flow diameter. While preserving workability is the main priority, RHA should be restricted to lower levels (<50%). Finally, VPP gives a notable improvement in workability compared to the control, even at high replacement levels of 50%.

3.2. Unit Weight

The results of the EGC unit weight tests are plotted in Figure 8. The unit weight of the control mixture was 2128 kg/m^3. By replacing the slag with either RHA or GWP, the unit weight gradually decreased. The EGC unit weight reached its lowest value at a 50% replacement ratio with a value of 1950 kg/m^3 in mixture RHA-50 (8.36% decrease) and a value of 2067 kg/m^3 in mixture GWP-50 (2.86% decrease). This decrease is attributed to the fact that both RHA and GWP have a lower density than the replaced slag. When replacing slag with VPP and when compared to the control mixture, it was found that the EGC unit weight increased with the replacement rate increase because the open-cell structure of VPP allows it to be easily filled and compacted, resulting in reduced porosity in the EGC mixture. This reduction in porosity leads to increased density compared to the EGC control mixture. In addition, the high reactivity of VPP with the alkaline activator contributes to a more compact and cohesive matrix and hence increased unit weight. Using 50% VPP increased the EGC unit weight to 2269 kg/m^3 (6.62% increase).

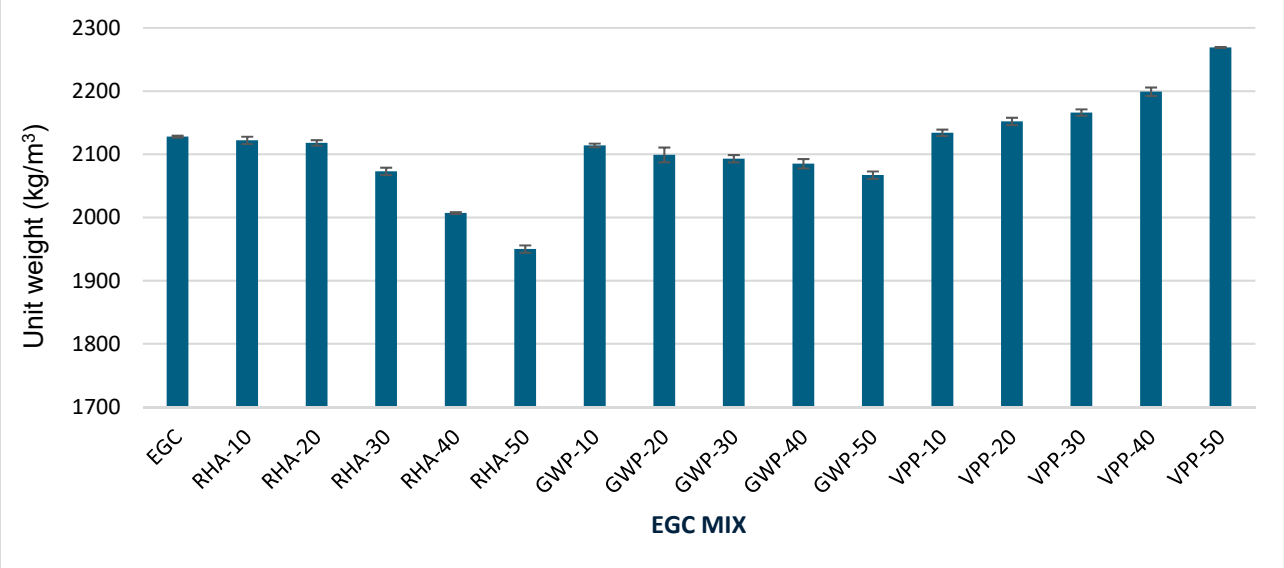

Figure 8. Unit weight of EGC.

In conclusion, unit weights for RHA and GWP drop with rising replacement rates until they achieve their lowest values at a 50% substitution level, whereas unit weights for VPP grow with increasing rates until they achieve their greatest values at a 50% substitution level.

3.3. Compressive Strength

All results are indicated in Table 4 and plotted in Figure 9. The control EGC mixture showed compressive strengths of 75, 78, and 79 MPa at 7, 28, and 56 days, respectively. When replacing slag with RHA/GWP/VPP, it was found that the compressive strength decreased at any given replacement ratio and EGC age compared to the control mixture. For example, at 28 days, replacing EGC slag by 10%, 20%, 30%, 40%, and 50%, decreased

its compressive strength by 26.9%, 21.8%, 16.7%, 32.1%, and 43.6%, respectively, when using RHA; by 29.3%, 16.7%, 32.1%, 30.8%, and 38.5%, respectively, when using GWP; and by 23.1%, 32.1%, 35.9%, 39.7%, and 46.2%, respectively, when using VPP. Within each group, the highest EGC compressive strength was shown at 30% RHA (65 MPa), 20% GWP (65 MPa), and 10% VPP (60 MPa), which reflect the optimal ratios to use for these waste materials as an EGC slag partial replacement. The mixtures with a larger slag content had higher compressive strengths because of the development of calcium silicate hydrates (C-S-H) and alumino-silicate hydrate (A-S-H) gel (phases and the density of the microstructure [40,41]. The decrease in EGC compressive strength when using RHA/GWP/VPP is attributed to several reasons. For RHA, increasing the RHA content causes an imbalance between Si and Al, which leads to the formation of low cross-linked aluminosilicates [8,42], which causes a decrease in compressive strength [38]. Zeyad et al. [43] pointed out that the compressive strength was significantly reduced when 15% of RHA was used in place of slag, which potentially led to a higher silica content. According to research of Patel and Shah [39], there is an optimal range of 5% to 10% for substituting RHA with slag. In addition, compared to the geopolymer matrix zero-RHA, it was shown that adding RHA in place of slag at replacement ratios between 15% and 25% resulted in a decrease in compressive strength. According to Kusbiantoro et al. [44], the strength decreased with increasing RHA content because the difference in slag and RHA's degrees of solubility decreases the rate at which aluminosilicate compounds dissolve and condense.

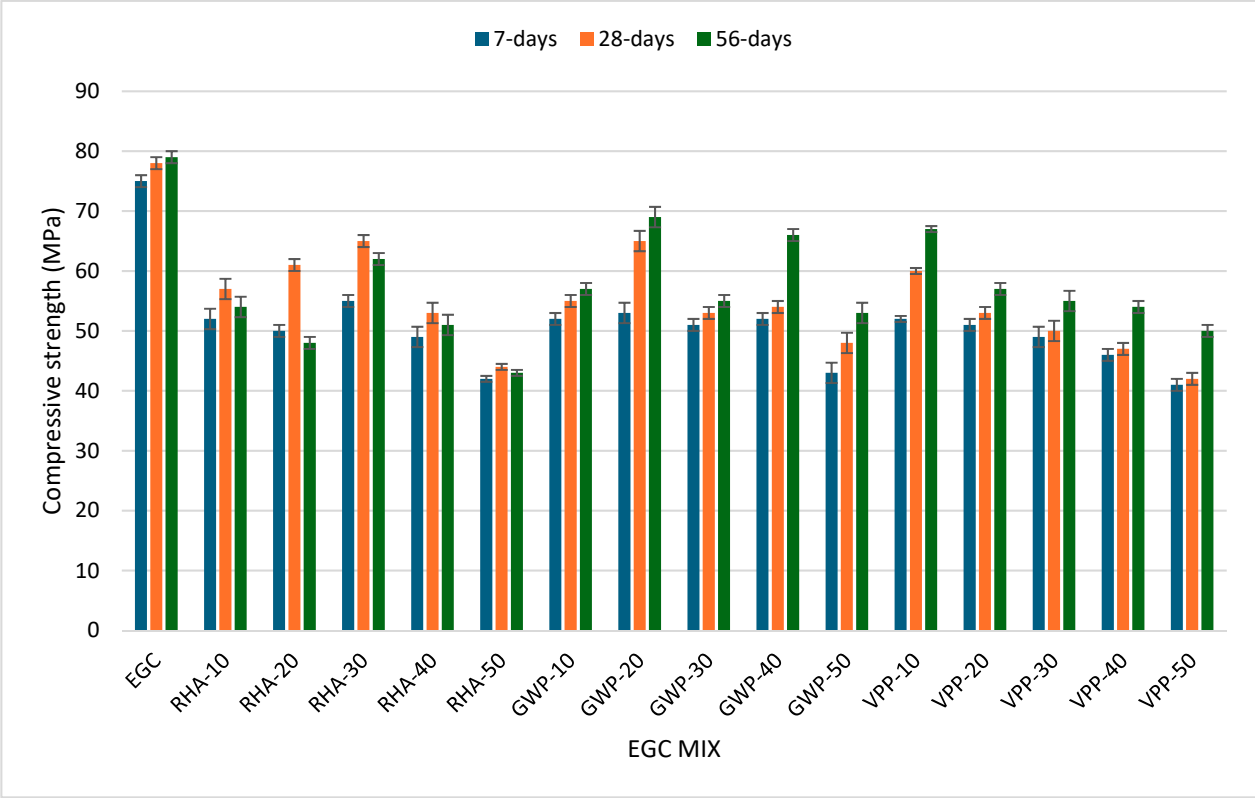

Figure 9. Compressive strength of EGC at different ages.

The excessive incorporation of GWP disrupted the geopolymer matrix formation and weakened the bond between particles, hence resulting in lower strength. Shilar et al. [27] concluded that the maximum compressive strengths were obtained with a GWP content of 20%. Khater et al. [45] concluded that a further increase in the content of granite waste powder of up to 15% causes the created geopolymer structure to deactivate and lose strength. The increased amounts of VPP decreased the compressive strength due to decreased Ca/Si ratio [46].

All EGC mixtures in this study showed common development of their compressive strength when comparing the 7, 28, and 56 days' strengths for each mixture, except for the RHA group. When using RHA as partial slag replacement in EGC, the compressive strength increased from age of 7 days to 28 days by 9.6%, 22%, 18.2%, 8.1%, and 4.7%, respectively, at 10%, 20%, 30%, 40%, and 50% RHA content; however, the corresponding strength of these mixtures decreased from an age of 28 days to 56 days by 5.2%, 21.3%, 4.6%, 3.7%, and 2.2%, respectively. This strength decrease at late EGC ages can be attributed to several reasons. The interaction between RHA and alkaline activators in the EGC mixture may be varied over time, affecting the geopolymerization process and strength development at different ages. It could also be due to moisture absorption, as RHA may have higher moisture absorption properties compared to slag, which may cause changes in the EGC matrix over time, affecting the compressive strength at 56 days. The temperature changes can be another reason why the temperature fluctuations during the curing period can affect the strength development of EGC, leading to differences in compressive strength at different ages. Future research is needed to focus on the RHA-based EGC strength development at late ages.

In conclusion, the optimum ratio regarding strength and material sustainability is 30% RHA replacement and 20% GWP, which maintains enough geopolymer matrix integrity while offering an acceptable degree of strength. Finally, 10% VPP substitution is recommended for higher strength requirements since higher VPP content results in significant strength losses.

3.4. Tensile Strength

As shown in Table 4 and Figure 10, the tensile strength of the EGC control mixture was 4.5 MPa, and when slag was replaced with RHA, the tensile strength ranged from 3.5 to 4.5 MPa. The RHA mixture with a 30% replacement ratio (RHA-30) obtained the highest tensile strength of 4.5 MPa, which is equal to the tensile strength of the control mixture. Beyond 30% RHA, the high substitution of slag decreased the tensile strength. Factors such as poor dispersion of RHA particles, increased porosity, or altered microstructure could lead to a decrease in the tensile strength of RHA mixtures. The tensile strength generally follows a similar trend with compressive strength, decreasing with higher slag replacement ratios. Mehta and Siddique [47] stated that the inclusion of RHA beyond 15% decreased split tensile strength. This was due to the difference in solubility rates of RHA and slag and the presence of unreactive silica in the mixture. Patel and Shah [39] show that when the content of RHA increases, split tensile strength decreases, and at all curing ages and at 100% slag content, the greatest split tensile strength values are obtained at ambient temperature.

When replacing slag with GWP at a rate of 10%, the tensile strength decreased by 11.1%, compared to the control mixture. Beyond that, the tensile strength increased by 24.4% and 8.8% at rates of 20% and 30% GWP, respectively. This is in contrast to what resulted in the compressive strength, in which it decreased at all replacement ratios compared to the control mixture. At 40% and 50% GWP, the EGC tensile strength decreased by 2.2% and 22.2%, respectively. The increase in tensile strength at 20% and 30% GWP may be due to the chemical composition of GWP, which enhances the reactions within the geopolymer matrix, resulting in stronger bond formation and increased tensile strength. Also, these replacement ratios may exhibit better compatibility with PP fibers, which improves the bonding between the fibers and the geopolymer matrix and, hence, provides better tensile strength. Shilar et al. [27] observed that with an increase in the GWP content in the mix, the split tensile strength increases up to 20% GWP; beyond 20%, the split tensile strength decreases.

The tensile strength decreased when VPP was used as a partial replacement of EGC slag by 2.2% to 37.8%, as it showed 4.4 MPa in mixture VPP-10 and 2.8 MPa in mixture VPP-50. The is attributed to the lower adhesion and bonding that might occur between the geopolymer matrix, fibers, and VPP particles, as is the case when slag was present at a high content, leading to weak bonding and decreased tensile strength. There is a clear

correlation between compressive and tensile strengths. Both strengths peak at optimum replacement ratios but decline significantly at higher replacement levels.

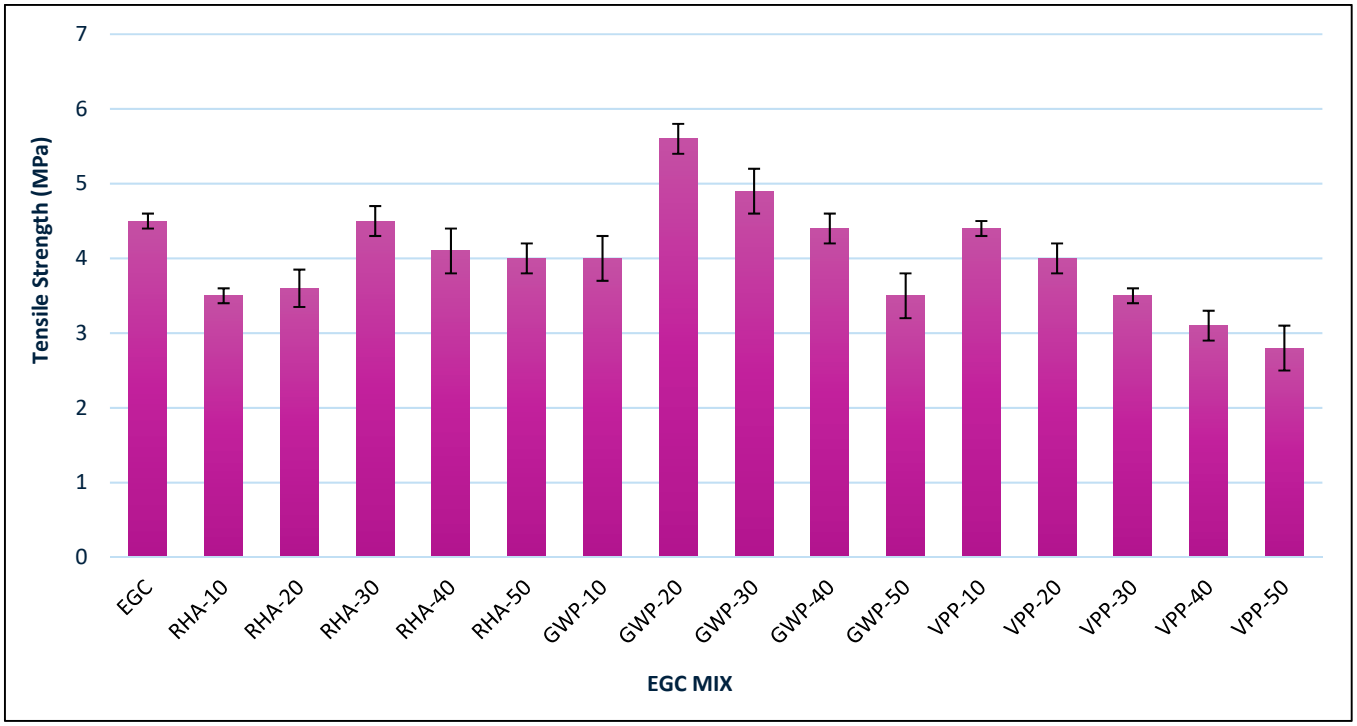

Figure 10. Tensile strength of EGC.

To sum up, according to the tensile strength data, the EGC mixes' tensile performance is greatly impacted when slag is substituted with RHA, GWP, or VPP. A 30% RHA replacement ratio provides an optimal tensile strength equal to the control mixture. The optimum balance is provided by 20% GWP substitution, which increases tensile strength by 24.4%. Since all VPP mixes resulted in a reduction in tensile performance, it is not advised to utilize VPP as a partial substitute for slag in order to increase tensile strength. Replacements of 30% RHA or 20% GWP are advised for situations where tensile strength is crucial since they provide optimum performance while still using sustainable resources.

3.5. Flexural Strength

All results are indicated in Table 4 and plotted in Figure 11.

The flexural strength of the EGC control mixture showed a value of 6 MPa. Using RHA in EGC showed a flexural strength trend similar to that of the corresponding tensile strength due to the strong correlation between them. The flexural strength increased with increasing RHA content until it reached its maximum value at the optimal replacement ratio of 30%, then decreased beyond that. The flexural strength decreased by 8.3% and 5% at 10% and 20% RHA, respectively, and increased by 3.3% at 30% RHA. It again decreased by 16.7% and 20% at 40% and 50% RHA, respectively. When using RHA that has a high SiO_2/Al_2O_3 ratio, the increase in the concentration of amorphous silica in the geopolymer structure may be the reason for the declining flexural strength. This occurrence produces a geopolymer gel with a lower flexural strength that is weaker, less densely bonded, and more porous. Moreover, the dissolution rate and polycondensation of aluminosilicates decreased due to the difference in melting points between GBFS and RHA. As a result, the strength decreases with the increase in RHA amount [43].

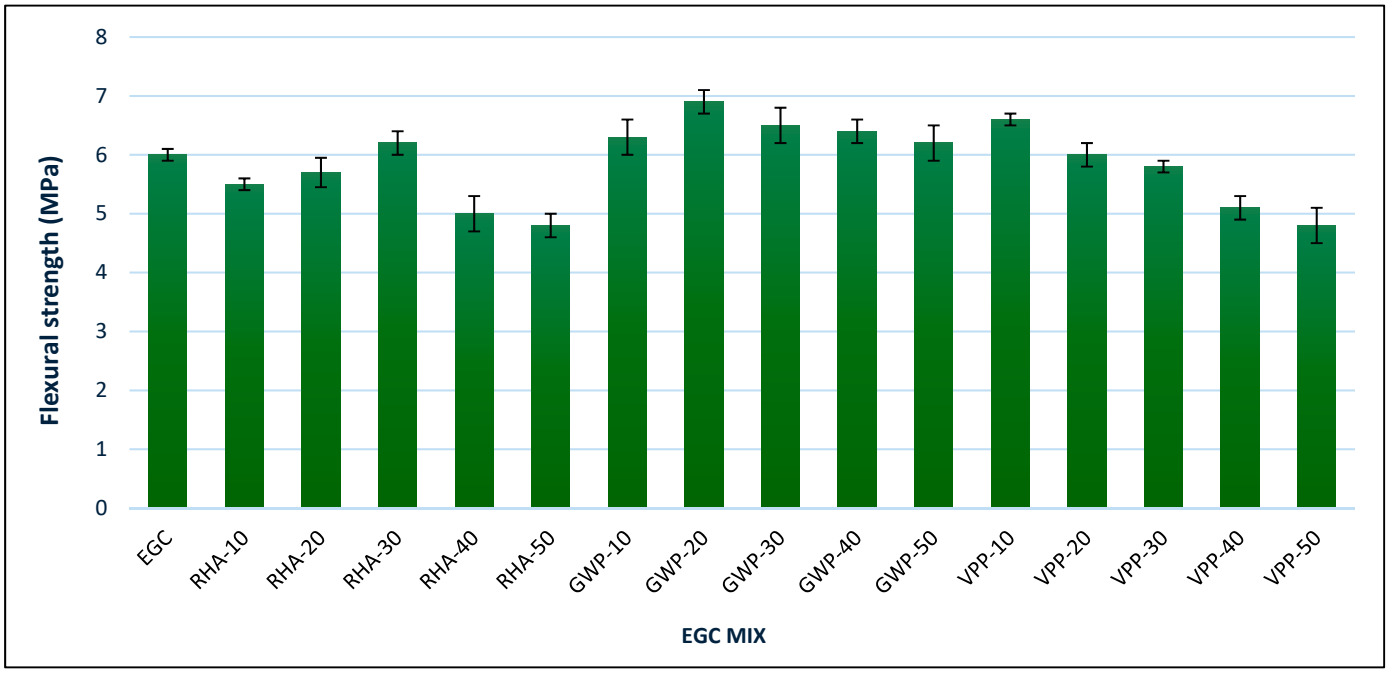

Figure 11. Flexural strength of EGC.

In all GWP mixtures, the flexural strength improved compared to the control mixture, where the maximum flexural strength was achieved at a replacement ratio of 20% with an increase of 15%. This is in contrast to what resulted in the compressive strength, in which it decreased at all replacement ratios compared to the control mixture, as well as the tensile strength, where the increase was at replacement ratios of 20% and 30% only. GWP has pozzolanic properties, reacting with the alkaline activators in the geopolymer matrix to form additional binding phases. This reaction led to the formation of more hydrated products, enhancing the interfacial transition zone between the fibers and the matrix, which improved the load transfer mechanism and flexural strength. In the same direction, Shilar et al. [27] found that the flexural strength increased with GWP levels up to 20%, but beyond 20%, the flexural strength decreased.

The flexural strength at 10% VPP increased by 10% due to the optimum pozzolanic activity, in which VPP actively participates in pozzolanic reactions, resulting in additional C-S-H and other binding phases. These reactions complemented the binding capacity of the geopolymer matrix and enhanced its overall strength. The additional hydrated products formed at this level also improved the adhesion between the fibers and the matrix and enhanced the load transfer mechanism and flexural strength. This is in contrast to what resulted in the compressive and tensile strengths, in which they decreased at all replacement ratios compared to the control mixture. At 20% VPP, the pozzolanic activity of VPP contributed positively to the geopolymer matrix, but the reduced GGBS content began to offset these benefits. GGBS is a major component of the geopolymer, and its low presence means that the matrix cannot benefit much from the improved properties of VPP alone, resulting in no significant gain or loss in flexural strength. As the VPP content increased by 30%, 40%, and 50%, the decrease in GGBS became significant, resulting in a weaker matrix that reduced the load transfer efficiency. This poor interaction resulted in decreased flexural strength.

In conclusion, 30% RHA is the optimum replacement ratio because it maximizes flexural strength; however, performance is adversely affected by larger RHA concentrations. Of all the replacement materials, a 20% GWP replacement ratio provides the maximum flexural strength and the best performance. While a 10% VPP substitution improves flexural strength, greater levels result in a weaker geopolymer matrix and worse performance. A 30% RHA or 20% GWP replacement is advised for increasing flexural strength; GWP

exhibits the best increase. To prevent appreciable decreases in matrix strength, VPP usage should be limited to tiny amounts.

3.6. Water Absorption and Apparent Porosity

The results of the water absorption and apparent porosity tests are shown in Table 4 and plotted in Figure 12. The water absorption and apparent porosity of the control EGC mixture were found to be 6.88% and 13.44%, respectively. When slag was replaced by RHA, the water absorption and apparent porosity increased with the increase in the RHA ratio. This is due to the increased porosity of RHA, which tends to have a more porous structure compared to slag. The RHA can absorb and retain water, which contributes to the increased water absorption of the composite. The water absorption of EGC containing RHA ranged from 7.49% to 14.18%, and the apparent porosity ranged from 14.42% to 23.54%. These results are consistent with the study of Zhao, Y. et al. [8] who concluded that RHA increased water absorption and the capillary absorption coefficient of geopolymer paste due to a great number of interrelated pores at a microscopic scale, resulting in RHA being able to absorb a huge amount of water.

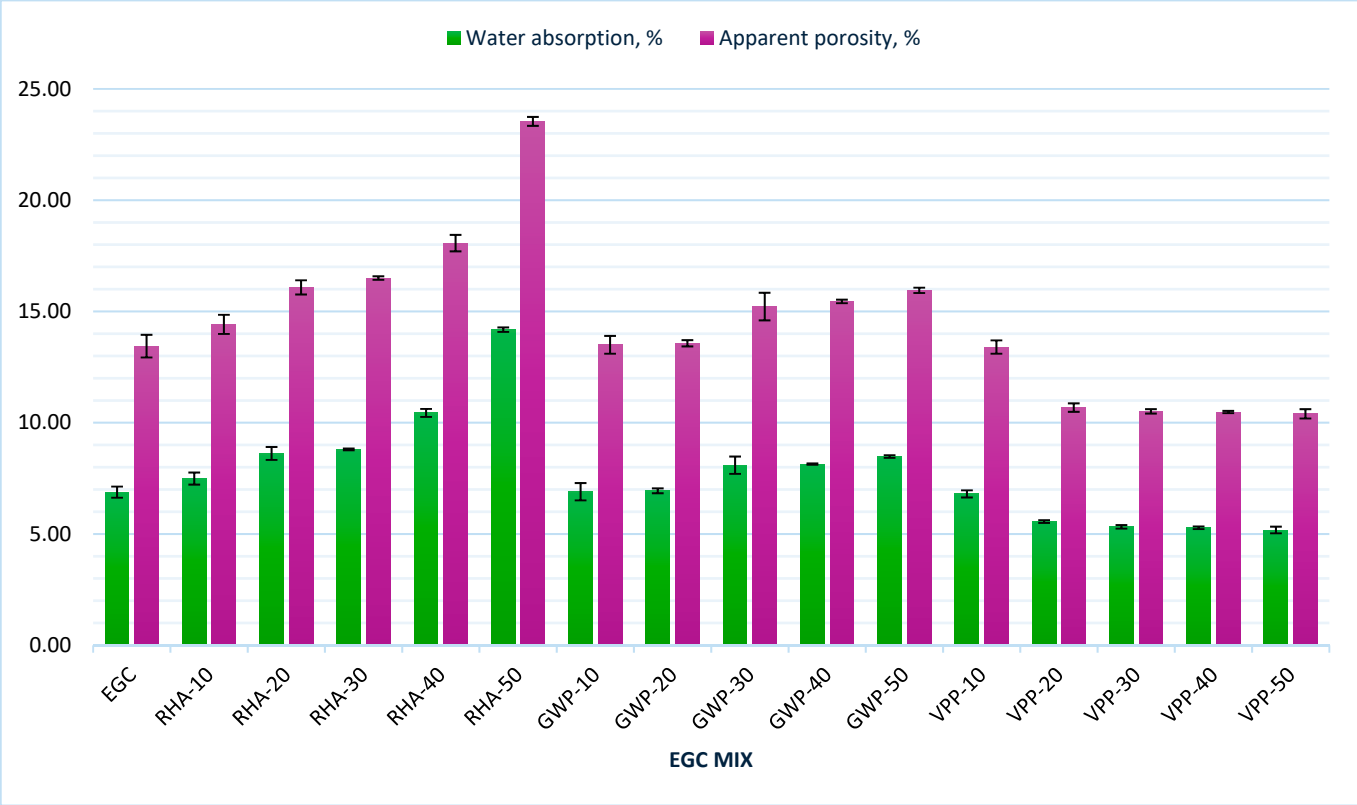

Figure 12. Water absorption and apparent porosity of EGC.

When slag was replaced by GWP, water absorption and apparent porosity increased with increasing GWP content compared to the control EGC mixture until reaching the highest water absorption and porosity of 8.48% and 15.95%, respectively, in the GWP-50 mixture. This increase is due to the larger particle size of GWP compared to slag, which led to less dense packing of particles within the geopolymer matrix, resulting in increased voids and, therefore, increased porosity and water absorption. A similar conclusion was obtained by Shilar et al. [27] in that water absorption increases as the proportion of granite increases.

The use of VPP showed a decrease in water absorption and porosity when compared to the control mixture. By increasing the VPP content, the water absorption and porosity kept decreasing, showing the lowest values of 5.18% and 10.4%, respectively, in the VPP-50 mixture. Since the open cell structure of VPP allows it to be easily filled and compacted,

it led to an increase in EGC density, a decrease in its porosity, and a decrease in water absorption. Zeyad et al. [48] showed that a pore's tortuosity increase with increasing volcanic pumice particles can significantly reduce permeability and water absorption. This result is consistent with the unit weight test results discussed in Section 3.2.

The results of water absorption and apparent porosity tests revealed a clear trend in which increasing RHA content consistently resulted in higher water absorption and porosity, highlighting its more porous nature than slag. This porous structure allowed for greater water retention, with the highest values observed at 50% RHA replacement. Similarly, increasing GWP concentration increased water absorption and porosity, resulting in greater voids in the geopolymer matrix. In contrast, VPP responded differently, in which increasing its concentration resulted in a reduction in water absorption and porosity, with the lowest values reported at 50% VPP.

3.7. Residual Compressive Strength

All results are indicated in Figure 13. At 200 °C, the residual compressive strength of the control EGC mixture decreased by 3.8% compared to that measured at room temperature. The irregular shape of the slag particles and its high density, which produces a dense mix, led to the accumulation of vapor pressure that caused crack formations and reduced the transition area between the EGC matrix and the PP fibers. This result is consistent with the unit weight test result discussed in Section 3.2. The mixtures containing the optimum replacement ratios (RHA-30, GWP-20, VPP-10) showed better resistance to high temperatures, as it improved by 4.6%, 20%, and 3.3% for mixtures RHA-30, GWP-20, and VPP-10, respectively, compared with that measured at room temperature. The improvement in strength at 200 °C temperature is the result of the further geopolymerization process between SF and slag in addition to the optimal substitute material ratio with the alkaline solution. The compressive strength decreased by 21.9%, 32.4%,12.2% and 23.1% for mixtures RHA-10, RHA-20, RHA-40 and RHA-50, respectively; by 16.3%, 10.3%,11.8%, and 2.7% for mixtures GWP-10, GWP-30, GWP-40, and GWP-50, respectively; and by 9.4%, 22%, 6.3%, and 13% for mixtures VPP-20, VPP-30, VPP-40, and VPP-50, respectively.

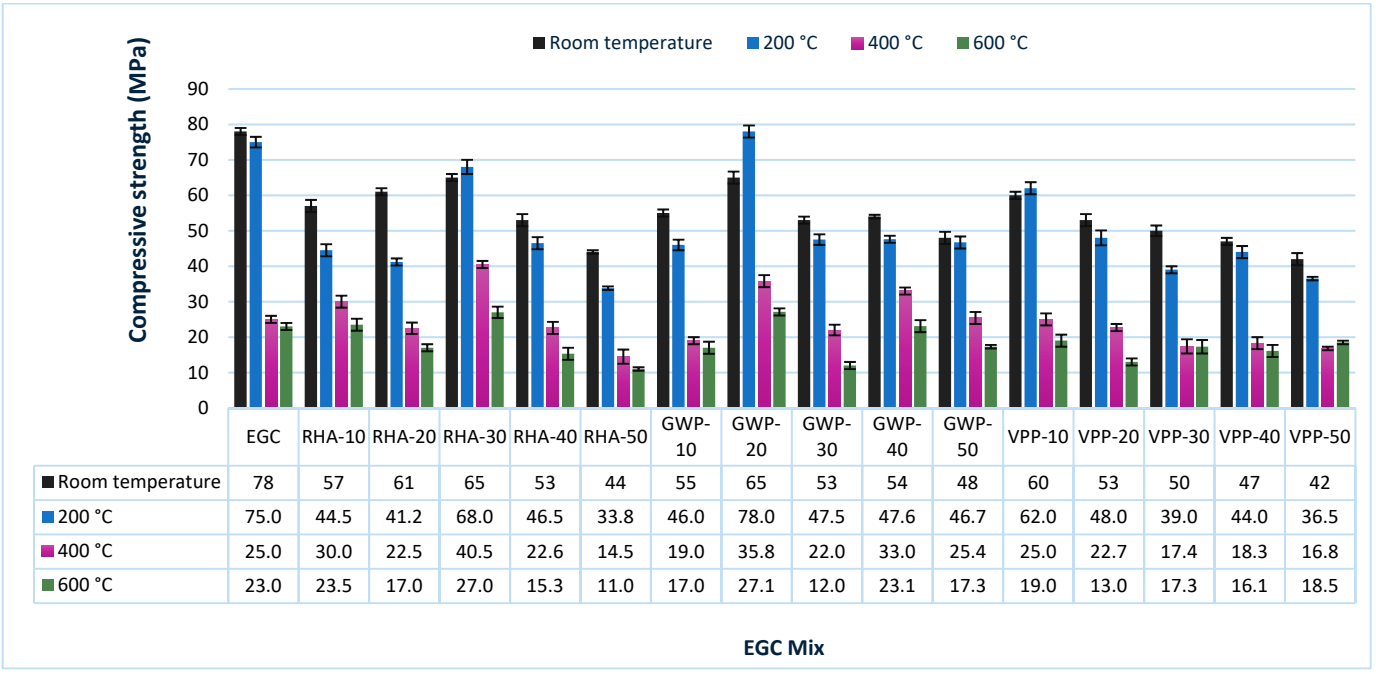

	EGC	RHA-10	RHA-20	RHA-30	RHA-40	RHA-50	GWP-10	GWP-20	GWP-30	GWP-40	GWP-50	VPP-10	VPP-20	VPP-30	VPP-40	VPP-50
Room temperature	78	57	61	65	53	44	55	65	53	54	48	60	53	50	47	42
200 °C	75.0	44.5	41.2	68.0	46.5	33.8	46.0	78.0	47.5	47.6	46.7	62.0	48.0	39.0	44.0	36.5
400 °C	25.0	30.0	22.5	40.5	22.6	14.5	19.0	35.8	22.0	33.0	25.4	25.0	22.7	17.4	18.3	16.8
600 °C	23.0	23.5	17.0	27.0	15.3	11.0	17.0	27.1	12.0	23.1	17.3	19.0	13.0	17.3	16.1	18.5

Figure 13. Residual compressive strength after exposure to high elevated temperatures.

At a temperature of 400 °C, the control mixture EGC witnessed a decrease in compressive strength of 67.9%, while the other mixtures had strength decrease of 47.4%, 63.1%,

37.7%, 57.4%, and 67.0% for mixtures RHA-10, RHA-20, RHA-30, RHA-40, and RHA-50, respectively; of 65.5%, 44.9%, 58.5%, 38.9%, 47.1% for mixtures GWP-10, GWP-20, GWP-30, GWP-40, and GWP-50, respectively; and of 58.3%, 57.2%, 65.2%, 61.1%, and 60% for mixtures VPP-10, VPP-20, VPP-30, VPP-40 and VPP-50, respectively.

At a temperature of 600 °C, the control mixture EGC witnessed a decrease in compressive strength by 70.5%, while the other mixtures had a strength decrease of 58.8%, 72.1%, 58.5%, 71.1%, and 75% for mixtures RHA-10, RHA-20, RHA-30, RHA-40, and RHA-50, respectively, of 69.1%, 58.3%, 77.4%, 57.2%, and 64% for mixtures GWP-10, GWP-20, GWP-30, GWP-40, and GWP-50, respectively; and of 68.3%, 75.5%, 65.4%, 65.7%, and 56% for mixtures VPP-10, VPP-20, VPP-30, VPP-40, and VPP-50, respectively.

The compressive strength decrease under high elevated temperature is attributed to the PP fiber's performance when subjected to high temperature. The melting point of these fibers is between 160 and 170 °C. These fibers start to melt and break down at 200 °C and above, which leaves continuous voids in the EGC matrix and reduces the mechanical characteristics.

There is a clear correlation between compressive strength and residual compressive strength under high temperatures. The mixtures with optimum replacement ratios (RHA-30, GWP-20, VPP-10) not only maintained higher compressive strength at room temperature but also showed superior resistance to strength loss when exposed to high temperatures.

In conclusion, at 200 °C, GWP-20 exhibited the highest increase in compressive strength (20%), followed by RHA-30 (4.6%) and VPP-10 (3.3%). At 400 °C and 600 °C, the compressive strength of all mixtures showed a significant decline. The melting and decomposition of PP fibers above 200 °C are the primary factors behind the reduced compressive strength across all mixtures at elevated temperatures. Among the mixtures, GWP-20 exhibited the smallest strength loss at both 400 °C and 600 °C, indicating better thermal resistance compared to other mixtures.

4. Microstructure Analysis

Figure 14 shows the SEM analysis results of the selected EGC mixes. As shown in Figure 14a, the EGC control mixture presents a compact and dense matrix with fewer microcracks and minimal porosity, in addition to very limited unreacted particles. This denser microstructure is attributed to the effective geopolymerization process. Thus, when the volume and permeability of the voids, pores, and cracks decrease, the compressive strengths of the EGC increase and their durability improves, as observed and discussed in Section 3. PP fibers are embedded within the matrix, enhancing the composite's mechanical properties by bridging microcracks and providing additional tensile strength. The interface between the fibers and the matrix appears to be well-bonded, indicating effective load transfer between the matrix and the fibers. This interaction is crucial for the composite's performance under tensile and flexural loads. Some microcracks are visible in the image, which can be attributed to the curing process or mechanical stresses. These microcracks can propagate under loading conditions, potentially affecting the composite's integrity.

Well-dispersed RHA particles within the matrix are shown in Figure 14b. Compared to the EGC mixture, the RHA-30 mixture exhibits more porosity and microcracks. These voids can lead to higher water absorption and apparent porosity, as evident by the measured relevant characteristics. On the other hand, homogenous microstructure can be seen in Figure 14c for mixture GPW-20, although some regions exhibit higher porosity. The presence of GWP can contribute to this variation in density. The interface between the PP fibers and the geopolymer matrix seems well-integrated, indicating good adhesion that is essential for effective stress transfer between the fibers and the matrix. Some microvoids and pores are also visible in the structure. These can impact the composite's mechanical properties and durability. The inclusion of GWP introduced additional porosity compared to the EGC control mixture. The dense regions in the image likely represent the CSH phase, which is formed by the reaction of GGBS and the alkaline activator. This phase is crucial for the compressive strength of the composite. The presence of GWP can increase the apparent porosity and water absorption of the composite. This is consistent with findings

in recent studies [49], where the incorporation of waste powders tends to introduce more porosity due to less efficient packing compared to EGC control mixtures. Figure 14d shows a dense matrix with embedded fibers when VPP was present, which indicates efficient geopolymerization and fiber distribution. The figure also shows that the volcanic pumice powder particles are completely dissolved and have reacted with the activator solution, resulting in the formation of a geopolymer grid.

In conclusion, better mechanical qualities are often associated with dense matrix structures and evenly distributed fibers, whereas increasing porosity tends to decrease strength and durability.

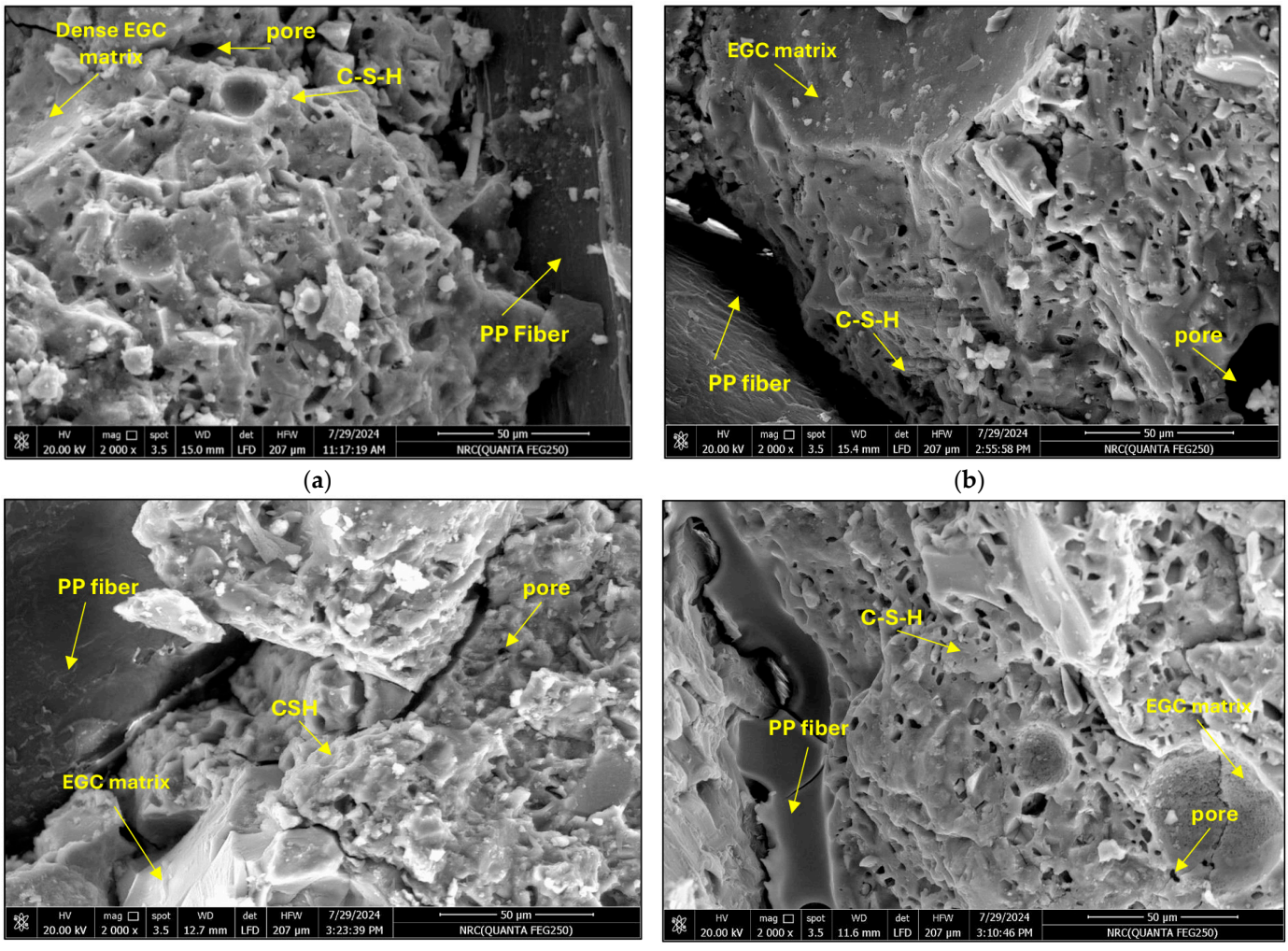

Figure 14. SEM images of EGC mixes: (**a**) EGC-control, (**b**) RHA-30, (**c**) GWP-20, and (**d**) VPP-10.

5. Conclusions

This research focused on producing a more sustainable and eco-friendly EGC made of cheaper and more common pozzolanic waste materials, namely RHA, GWP, and VPP. These waste materials were used as partial substitutions (10–50%) of GGBFS in EGC. The effects of these wastes on the mechanical, durability, and microstructure properties were examined. The following key conclusions can be listed:

1. Using RHA or GWP generally decreased the EGC workability by up to 31%, However, using VPP in EGC increased its workability by up to 38%. The compressive strength decreased by up to 43.6% when using RHA, 38.5% when using GWP, and 46.2% when using VPP compared to the control mixture at 28 days. Optimal replacement ratios were identified as 30% for RHA, 20% for GWP, and 10% for VPP.

2. Increasing GWP content led to higher water absorption and apparent porosity, reaching 8.48% and 15.95%, respectively, at a 50% replacement ratio. In contrast, using VPP reduced water absorption and porosity.
3. At 200 °C, optimal mixtures (RHA-30, GWP-20, VPP-10) showed improved strength, while other mixtures exhibited substantial strength decreases. At 400 °C and 600 °C, all mixtures experienced significant strength reductions. For applications requiring high-temperature resistance, high-melting point refractory fibers used to replace low-melting point polypropylene fibers tend to melt and decompose at elevated temperatures.
4. The SEM analysis of the control EGC mixture exhibited a dense matrix with minimal porosity and well-bonded PP fibers, contributing to enhanced mechanical properties. In the RHA-30 mixture, increased porosity and microcracks were observed. The GWP-20 mixture showed a homogeneous microstructure but with higher porosity. The VPP-10 mixture displayed efficient geopolymerization with a dense matrix and well-distributed fibers.
5. It is recommended for future studies to investigate other durability properties of EGC, such as chloride permeability, sulfuric acid attacks, dry shrinkage, freezing, and corrosion. It is also recommended to focus on investigating the strength development of RHA-based EGC at late ages.

Author Contributions: Conceptualization, A.M.T. and O.Y.; methodology, A.M.T., D.S.A., M.A. and O.Y.; validation, D.S.A. and M.A.; investigation, A.M.T., D.S.A. and O.Y.; data curation, D.S.A.; writing—original draft, D.S.A.; writing—review and editing, A.M.T. and O.Y.; visualization, M.A. and O.Y.; supervision, A.M.T. All authors have read and agreed to the published version of the manuscript.

Funding: This research received no external funding.

Data Availability Statement: The original contributions presented in the study are included in the article. Further inquiries can be directed to the corresponding author.

Conflicts of Interest: The authors declare no conflict of interest.

References

1. Biyani, Y.; Patil, L.G.; Kurhe, C.N. *Engineered Cementitious Composites*; Springer International Publishing: Berlin/Heidelberg, Germany, 2020; Volume 2, ISBN 9783662584378.
2. Stark, J.; Möser, B.; Bellmann, F. *Nucleation and Growth of C-S-H Phases on Mineral Admixtures*; Springer: Berlin/Heidelberg, Germany, 2007; ISBN 9783540724476.
3. Wang, S.; Li, V. Engineered Cementitious Composites with High-Volume Fly Ash. *ACI Mater. J.* **2007**, *104*, 233–241. [CrossRef]
4. Andrew, R.M. Global CO_2 Emissions from Cement Production. *Earth Syst. Sci. Data* **2018**, *10*, 195–217. [CrossRef]
5. Luukkonen, T.; Abdollahnejad, Z.; Yliniemi, J.; Kinnunen, P.; Illikainen, M. One-Part Alkali-Activated Materials: A Review. *Cem. Concr. Res.* **2018**, *103*, 21–34. [CrossRef]
6. Aghaeipour, A.; Madhkhan, M.; Ashrafian, A.; Taheri Amiri, M.J.; Masoumi, P.; Asadi-Shiadeh, M.; Yaghoubi-Chenari, M.; Mosavi, A.; Nabipour, N.; Pavan, S.; et al. *Geopolymers Structure, Processing, Properties and Industrial Applications*; Woodhead Puplishing Limited: Cambridge, UK, 2017; Volume 21, ISBN 9789400776715.
7. Elemam, W.E.; Tahwia, A.M.; Abdellatief, M.; Youssf, O.; Kandil, M.A. Durability, Microstructure, and Optimization of High-Strength Geopolymer Concrete Incorporating Construction and Demolition Waste. *Sustainability* **2023**, *15*, 15832. [CrossRef]
8. Zhao, Y.; Chen, B.; Duan, H. Effect of Rice Husk Ash on Properties of Slag Based Geopolymer Pastes. *J. Build. Eng.* **2023**, *76*, 107035. [CrossRef]
9. Youssf, O.; Mills, J.E.; Elchalakani, M.; Alanazi, F.; Yosri, A.M. Geopolymer Concrete with Lightweight Fine Aggregate: Material Performance and Structural Application. *Polymers* **2023**, *15*, 171. [CrossRef]
10. Walkley, B. Geopolymers. *Encycl. Earth Sci. Ser.* **2020**, *37*, 1633–1656. [CrossRef]
11. Youssf, O.; Elchalakani, M.; Hassanli, R.; Roychand, R.; Zhuge, Y.; Gravina, R.J.; Mills, J.E. Mechanical Performance and Durability of Geopolymer Lightweight Rubber Concrete. *J. Build. Eng.* **2022**, *45*, 103608. [CrossRef]
12. Zhong, H.; Zhang, M. Engineered Geopolymer Composites: A State-of-the-Art Review. *Cem. Concr. Compos.* **2023**, *135*, 104850. [CrossRef]
13. Wang, F.; Ding, Y.; Nishiwaki, T.; Zhang, Z.; Yu, J.; Yu, K. Fully Recycled Engineered Geopolymer Composite: Mechanical Properties and Sustainability Assessment. *J. Clean. Prod.* **2024**, *471*, 143382. [CrossRef]

14. Behzad, N.; Jay, S.; Uddin, A.S.F. Tensile Strain Hardening Behavior of PVA Fiber-Reinforced Engineered Geopolymer Composite. *J. Mater. Civ. Eng.* **2015**, *27*, 4015001. [CrossRef]
15. Nematollahi, B.; Sanjayan, J.; Shaikh, F.U.A. Matrix Design of Strain Hardening Fiber Reinforced Engineered Geopolymer Composite. *Compos. Part B Eng.* **2016**, *89*, 253–265. [CrossRef]
16. Nematollahi, B.; Sanjayan, J. Effect of Different Superplasticizers and Activator Combinations on Workability and Strength of Fly Ash Based Geopolymer. *Mater. Des.* **2014**, *57*, 667–672. [CrossRef]
17. Nematollahi, B.; Sanjayan, J.; Shaikh, F.U.A. Synthesis of Heat and Ambient Cured One-Part Geopolymer Mixes with Different Grades of Sodium Silicate. *Ceram. Int.* **2015**, *41*, 5696–5704. [CrossRef]
18. Alrefaei, Y.; Dai, J.G. Tensile Behavior and Microstructure of Hybrid Fiber Ambient Cured One-Part Engineered Geopolymer Composites. *Constr. Build. Mater.* **2018**, *184*, 419–431. [CrossRef]
19. Ling, Y.; Wang, K.; Li, W.; Shi, G.; Lu, P. Effect of Slag on the Mechanical Properties and Bond Strength of Fly Ash-Based Engineered Geopolymer Composites. *Compos. Part B Eng.* **2019**, *164*, 747–757. [CrossRef]
20. Deb, P.S.; Nath, P.; Sarker, P.K. The Effects of Ground Granulated Blast-Furnace Slag Blending with Fly Ash and Activator Content on the Workability and Strength Properties of Geopolymer Concrete Cured at Ambient Temperature. *Mater. Des.* **2014**, *62*, 32–39. [CrossRef]
21. Ahmed, J.K.; Atmaca, N.; Khoshnaw, G.J. Exploring Flexural Performance and Abrasion Resistance in Recycled Brick Powder-Based Engineered Geopolymer Composites. *Beni-Suef Univ. J. Basic Appl. Sci.* **2024**, *13*, 68. [CrossRef]
22. Wu, H.; Liu, X.; Wang, C.; Zhang, Y.; Ma, Z. Micro-Properties and Mechanical Behavior of High-Ductility Engineered Geopolymer Composites (EGC) with Recycled Concrete and Paste Powder as Green Precursor. *Cem. Concr. Compos.* **2024**, *152*, 105672. [CrossRef]
23. Nair, D.G.; Jagadish, K.S.; Fraaij, A. Reactive Pozzolanas from Rice Husk Ash: An Alternative to Cement for Rural Housing. *Cem. Concr. Res.* **2006**, *36*, 1062–1071. [CrossRef]
24. Zabihi, S.M.; Tavakoli, H.R. Evaluation of Monomer Ratio on Performance of GGBFS-RHA Alkali-Activated Concretes. *Constr. Build. Mater.* **2019**, *208*, 326–332. [CrossRef]
25. Elyamany, H.E.; Abd Elmoaty, A.E.M.; Mohamed, B. Effect of Filler Types on Physical, Mechanical and Microstructure of Self Compacting Concrete and Flow-Able Concrete. *Alex. Eng. J.* **2014**, *53*, 295–307. [CrossRef]
26. Gautam, L.; Jain, J.K.; Kalla, P.; Danish, M. Engineered Cementitious Composites (ECC). *Mater. Today Proc.* **2020**, *44*, 4196–4203. [CrossRef]
27. Shilar, F.A.; Ganachari, S.V.; Patil, V.B.; Nisar, K.S.; Abdel-Aty, A.H.; Yahia, I.S. Evaluation of the Effect of Granite Waste Powder by Varying the Molarity of Activator on the Mechanical Properties of Ground Granulated Blast-Furnace Slag-Based Geopolymer Concrete. *Polymers* **2022**, *14*, 306. [CrossRef]
28. Zeyad, A.M.; Magbool, H.M.; Tayeh, B.A.; Garcez de Azevedo, A.R.; Abutaleb, A.; Hussain, Q. Production of Geopolymer Concrete by Utilizing Volcanic Pumice Dust. *Case Stud. Constr. Mater.* **2022**, *16*, e00802. [CrossRef]
29. Kabay, N.; Mert, M.; Miyan, N.; Omur, T. Pumice as Precursor in Geopolymer Paste and Mortar. *J. Civ. Eng. Constr.* **2021**, *10*, 225–236. [CrossRef]
30. *ASTM C 494/C 494M–17*; Standard Specification for Chemical Admixtures for Concrete. ASTM: West Conshohocken, PA, USA, 2000; Volume 8, pp. 3–4. [CrossRef]
31. Dong, M.; Feng, W.; Elchalakani, M.; Li, G.; Karrech, A.; May, E.F. Development of a High Strength Geopolymer by Novel Solar Curing. *Ceram. Int.* **2017**, *43*, 11233–11243. [CrossRef]
32. *AS 1012.3.5:2015*; Methods of Testing Concrete Method 3.5: Determination of Properties Related to the Consistency of Concrete—Slump Flow, T 500 and J-Ring Test. Australian Standard: Sydney, Australia, 2015; pp. 1–13.
33. *ASTM C 109*; Standard Test Method for Compressive Strength of Hydraulic Cement Mortars. ASTM International: West Conshohocken, PA, USA, 2020; Volume 4, p. 9.
34. Rokugo, K.; Yokota, H.; Sakata, N.; Kanda, T. "Recommendations for Design and Construction of High Performance Fiber Reinforced Cement Composite with Multiple Fine Cracks" Published by JSCE. *Concr. J.* **2007**, *45*, 3–9. [CrossRef]
35. *ASTM: C 1609/C 1609M–07*; Standard Test Method for Flexural Performance of Fiber-Reinforced Concrete. ASTM: West Conshohocken, PA, USA, 2007; pp. 1–9.
36. *ASTM C948-81*; Standard Test Method for Dry and Wet Bulk Density, Water Absorption, and Apparent Porosity. ASTM International: West Conshohocken, PA, USA, 1981; Volume 81, p. 2.
37. Givi, A.N.; Rashid, S.A.; Aziz, F.N.A.; Salleh, M.A.M. Assessment of the Effects of Rice Husk Ash Particle Size on Strength, Water Permeability and Workability of Binary Blended Concrete. *Constr. Build. Mater.* **2010**, *24*, 2145–2150. [CrossRef]
38. Das, S.K.; Mishra, J.; Singh, S.K.; Mustakim, S.M.; Patel, A.; Das, S.K.; Behera, U. Characterization and Utilization of Rice Husk Ash (RHA) in Fly Ash—Blast Furnace Slag Based Geopolymer Concrete for Sustainable Future. *Mater. Today Proc.* **2020**, *33*, 5162–5167. [CrossRef]
39. Patel, Y.J.; Shah, N. Enhancement of the Properties of Ground Granulated Blast Furnace Slag Based Self Compacting Geopolymer Concrete by Incorporating Rice Husk Ash. *Constr. Build. Mater.* **2018**, *171*, 654–662. [CrossRef]
40. Safari, Z.; Kurda, R.; Al-Hadad, B.; Mahmood, F.; Tapan, M. Mechanical Characteristics of Pumice-Based Geopolymer Paste. *Resour. Conserv. Recycl.* **2020**, *162*, 105055. [CrossRef]

41. Kotop, M.A.; El-Feky, M.S.; Alharbi, Y.R.; Abadel, A.A.; Binyahya, A.S. Engineering Properties of Geopolymer Concrete Incorporating Hybrid Nano-Materials. *Ain Shams Eng. J.* **2021**, *12*, 3641–3647. [CrossRef]
42. Abbas, I.S.; Abed, M.H.; Canakci, H. Development and Characterization of Eco- and User-Friendly Grout Production via Mechanochemical Activation of Slag/Rice Husk Ash Geopolymer. *J. Build. Eng.* **2023**, *63*, 105336. [CrossRef]
43. Zeyad, A.M.; Bayraktar, O.Y.; Tayeh, B.A.; Öz, A.; Özkan, İ.G.M.; Kaplan, G. Impact of Rice Husk Ash on Physico-Mechanical, Durability and Microstructural Features of Rubberized Lightweight Geopolymer Composite. *Constr. Build. Mater.* **2024**, *427*, 136265. [CrossRef]
44. Kusbiantoro, A.; Nuruddin, M.F.; Shafiq, N.; Qazi, S.A. The Effect of Microwave Incinerated Rice Husk Ash on the Compressive and Bond Strength of Fly Ash Based Geopolymer Concrete. *Constr. Build. Mater.* **2012**, *36*, 695–703. [CrossRef]
45. Khater, H.M.; El Nagar, A.M.; Ezzat, M.; Lottfy, M. Fabrication of Sustainable Geopolymer Mortar Incorporating Granite Waste. *Compos. Mater. Eng.* **2020**, *2*, 1–12.
46. Talaat Mohammed, D.; Yaltay, N. Strength and Elevated Temperature Resistance Properties of the Geopolymer Paste Produced with Ground Granulated Blast Furnace Slag and Pumice Powder. *Ain Shams Eng. J.* **2024**, *15*, 102483. [CrossRef]
47. Mehta, A.; Siddique, R. Sustainable Geopolymer Concrete Using Ground Granulated Blast Furnace Slag and Rice Husk Ash: Strength and Permeability Properties. *J. Clean. Prod.* **2018**, *205*, 49–57. [CrossRef]
48. Zeyad, A.M.; Tayeh, B.A.; Yusuf, M.O. Strength and Transport Characteristics of Volcanic Pumice Powder Based High Strength Concrete. *Constr. Build. Mater.* **2019**, *216*, 314–324. [CrossRef]
49. Luo, Y.; Bao, S.; Liu, S.; Zhang, Y.; Li, S.; Ping, Y. Enhancing Reactivity of Granite Waste Powder toward Geopolymer Preparation by Mechanical Activation. *Constr. Build. Mater.* **2024**, *414*, 134981. [CrossRef]